

Supplementary Information

Effects of high-shear mixing and graphene oxide weight fraction on the electrochemical properties of GO/Ni(OH)₂ electrode

Yinan Yuan ^a, Zhaoyuan Liu ^a, Bing Wei ^b, Ziyue Yang ^a, Lidong Wang ^{a, *}, Weidong Fei ^{a, *}

^a School of Materials Science and Engineering, Harbin Institute of Technology, Harbin 150001, China

^b School of Materials Science and Engineering, Heilongjiang University of Science and Technology, Harbin 150001, China

* Corresponding author.

Institute of Technology, Harbin, 150001, China.

E-mail address: wld@hit.edu.cn (L. Wang), wdfei@hit.edu.cn (W. Fei).

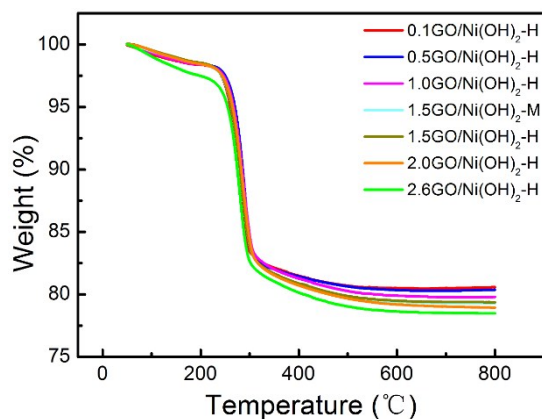


Figure S1 TGA curves of GO/Ni(OH)₂-M and GO/Ni(OH)₂-H with different GO volume fractions.

The thermo gravimetry analysis (TGA) was conducted on a TGA/SDTA851e analyser from 50 °C upon heating to 800 °C at a rate of 10 °C min⁻¹ under air atmosphere. A total weight loss of xGO/Ni(OH)₂-H were approximately to be 19.52%, 19.81%, 20.20%, 20.68%, 21.07% and 21.56% respectively, and xGO/Ni(OH)₂-M was approximately to be 20.64%. The weight fractions of GO can be calculated from the weight fractions of Ni(OH)₂ calculated from the weight fractions of NiO. So the weight fractions of GO in xGO/Ni(OH)₂-H were calculated to be 0.11%, 0.45%, 0.95%, 1.54%, 2.02%, 2.62%, respectively. The weight fractions of GO in xGO/Ni(OH)₂-M were calculated to be 1.48%. Accordingly, we named the composites xGO/Ni(OH)₂-H and xGO/Ni(OH)₂-M as 0.1GO/Ni(OH)₂-H, 0.5GO/Ni(OH)₂-H, 1.0GO/Ni(OH)₂-H, 1.5GO/Ni(OH)₂-H, 2.0GO/Ni(OH)₂-H, 2.6GO/Ni(OH)₂-H and 1.5GO/Ni(OH)₂-M, respectively.

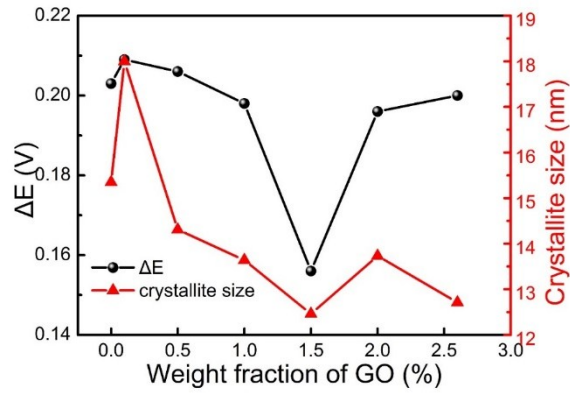


Figure S2 The relationship between peak potential separation (ΔE) and crystallite size of $\text{Ni}(\text{OH})_2\text{-H}$ perpendicular to (100) lattice plane for different weight fractions of GO in $\text{GO}/\text{Ni}(\text{OH})_2\text{-H}$.

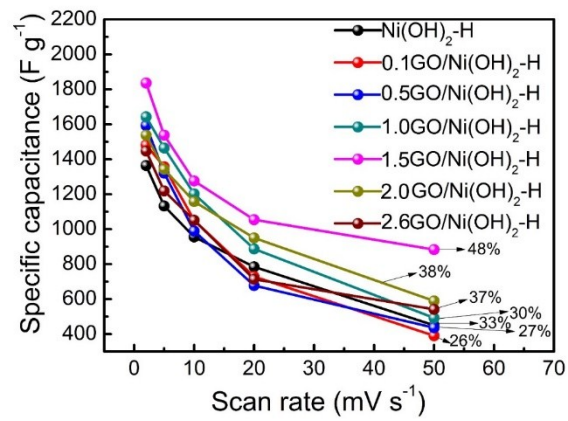


Figure S3 Specific capacitances of the $\text{Ni}(\text{OH})_2\text{-H}$ and $\text{GO}/\text{Ni}(\text{OH})_2\text{-H}$ with different weight fraction of GO at different scan rates.

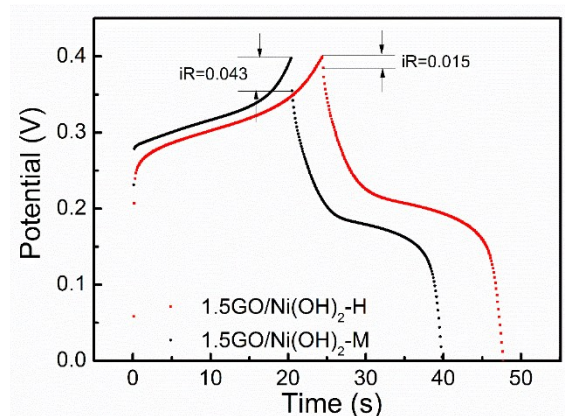


Figure S4 the iR drop of 1.5GO/Ni(OH)₂-H and 1.5GO/Ni(OH)₂-M at 20A g⁻¹.

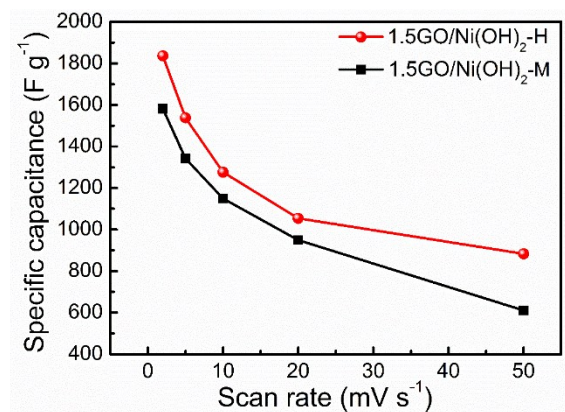


Figure S5 the specific capacitances of 1.5GO/Ni(OH)₂-H and 1.5GO/Ni(OH)₂-M under typical scan rates.

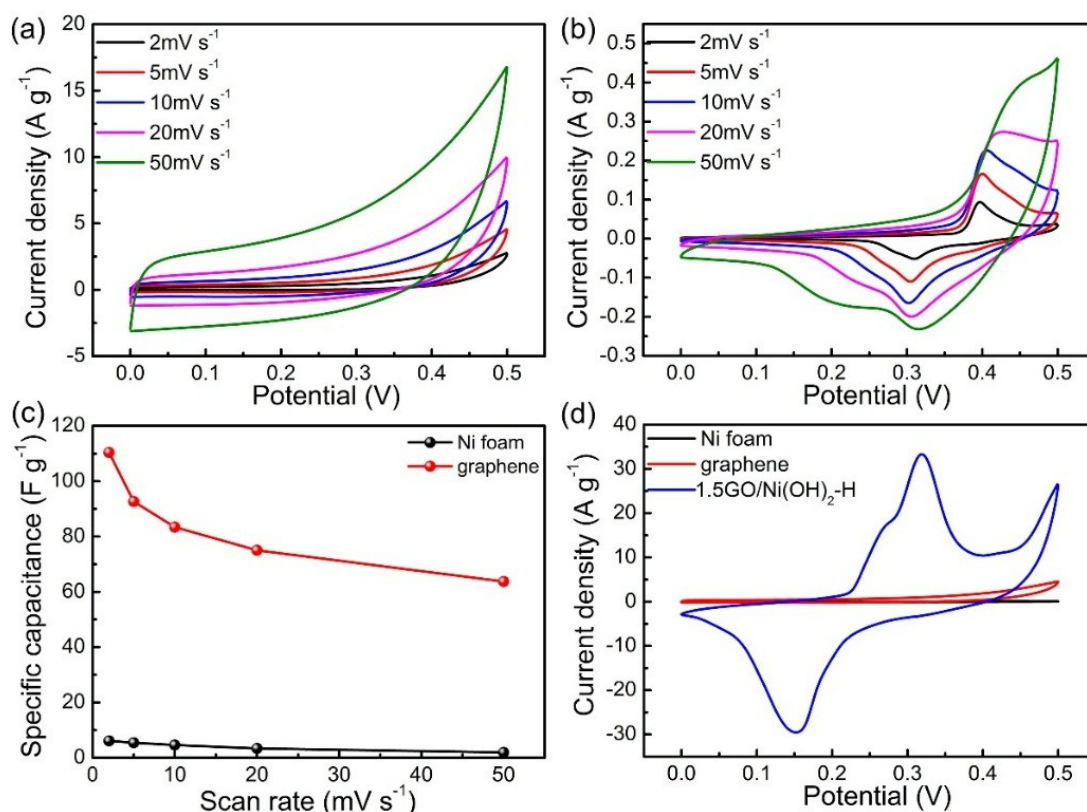


Figure S6 (a) the CV curves of RGO at different scan rates, (b) the CV curves of Ni foam at different scan rates, (c) the specific capacitances of RGO and Ni foam at different scan rates, (d) the CV curves of Ni foam, RGO and 1.5GO/Ni(OH)₂-H at scan rate of 5 mV s⁻¹.

The CV curves of RGO at different scan rates have tested and shown in Figure S6. The CV curves of RGO are shown in Figure S6a. The specific capacitances of RGO (in Figure S6c) are 110.4, 92.6, 83.4, 75.0 and 63.8 F g⁻¹ at scan rates of 2, 5, 10, 20 and 50 mV s⁻¹, respectively. The CV curves of Ni foam at different scan rates are shown in Figure S6b, and the specific capacitances of Ni foam (in Figure S6c) are 6.1, 5.4, 4.6, 3.4 and 1.9 F g⁻¹ at scan rates of 2, 5, 10, 20 and 50 mV s⁻¹, respectively. The specific capacitances of RGO are much larger than those of Ni foam at every scan rates. Figure S6d shows the CV curves of Ni foam, RGO and 10GO/Ni(OH)₂-H at scan rate of 5 mV s⁻¹. The specific capacitance of 10GO/Ni(OH)₂-H (1538 F g⁻¹) is much higher than that

of RGO (92.64 F g^{-1}) and Ni foam (5.4 F g^{-1}) at 5 mV s^{-1} . This results could confirm the current collector itself has a negligible capacitive contribution.

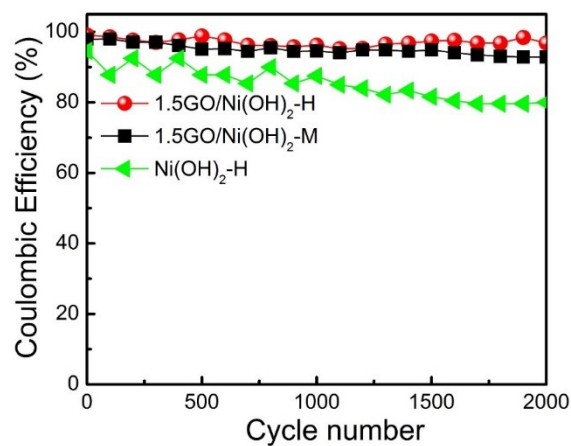


Figure S7 Coulombic efficiency of the Ni(OH)₂-H, 1.5GO/Ni(OH)₂-H and 1.5GO/Ni(OH)₂-M

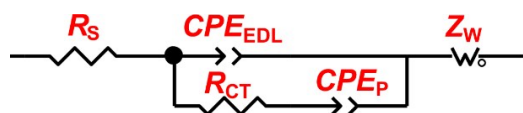


Figure S8 The equivalent electric circuit model used for fitting the Nyquist plots. R_s : the intrinsic ohmic resistance; R_{ct} : charge transfer resistance; CPE_{EDL} : constant phase element representing the electrical double layer capacitance (EDLC); CPE_p : constant phase element representing the pseudocapacitance provided by the oxygen functional groups; Z_w : a Generalized Finite Warburg element terminating in an open circuit.